Study on Ultra-Long-Distance Transportable Concentration Gradient of Coal Gangue Slurry with Different Gradations

Shi Wang [1,2], Haigen Yu [1,2], Rui Wu [1,2,*], Mingkun Tang [1,2], Yaohua Liu [1,2], Long Liu [1,2] and Xuepeng Song [3]

1   School of Resources and Environmental Engineering, Jiangxi University of Science and Technology, Ganzhou 341000, China; wangshi@jxust.edu.cn (S.W.); haigenyu@163.com (H.Y.); t_13247970762@163.com (M.T.); 15679790193@163.com (Y.L.); 13617068238@163.com (L.L.)
2   Key Laboratory of Mining Engineering of Jiangxi Province, Jiangxi University of Science and Technology, Ganzhou 341000, China
3   School of Energy and Mining Engineering, China University of Mining and Technology (Beijing), Beijing 100083, China; sxp9612@126.com
*   Correspondence: wurui@jxust.edu.cn; Tel.: +86-138-7070-1581

Abstract: Coal gangue, the primary solid waste generated during the coal mining process, is typically disposed of on the surface, where it gradually accumulates to form gangue piles that significantly contaminate the surrounding environment. Filling technology has been widely employed for the safe and efficient disposal of coal gangue due to its sustainability, safety, and efficiency. However, there is still a lack of theoretical research on the concentration of gangue slurry in long-distance filling pipeline transportation. Therefore, a calculation model of the ultra-long-distance transportable concentration of coal gangue slurry with different grades was constructed based on the static anti-segregation performance and Bingham model. In addition, the relevant parameters of the calculation model of the ultra-long-distance transportable concentration of coal gangue slurry in this mine were determined using the 8 km pipeline transport of coal gangue slurry in one mine as the technical background. It was subsequently demonstrated that the yield stress, plastic viscosity, and mass concentration of the various grades of gangue slurry in this mine exhibit an increasing exponential function, while the slurry density and mass concentration exhibit an increasing linear function, and the mass concentration and actual flow rate correspond to a quadratic polynomial increment. Finally, the minimum and maximum concentrations for different grades of gangue slurry that can be transported over long distances in this mine were determined. This work provides theoretical and practical guidance on how to select the concentration of gangue slurry for long-distance pipeline transport.

Keywords: coal gangue slurry; grading; pipeline transportation; rheological properties; concentration gradient

1. Introduction

For a long time, coal has been the cornerstone of China's strategic energy security system and will still play a role in energy security in the future [1–3]. The large-scale, high-intensity mining of coal resources will not only produce a large amount of coal gangue but also induce damage to the geological conditions and ecological environment of the mining area [4–8]. The state and the government have long been clearly required to improve the comprehensive utilization rate of coal gangue, but at present, they still mainly rely on the ground piling up or landfills. The problem of coal gangue disposal has gradually become a constraint on China's efficient development of mineral resources [9–11], and an ecological environmental protection strategy is one of the obstacles [12–15]. How to efficiently, greenly, scientifically, and safely dispose of solid wastes such as coal gangue will inevitably become the key to the realization of an ecological environment and the economic and social development of high quality in the field of coal [16–26].

To date, the application of gangue in the field of filling has attracted considerable attention, particularly in the context of ground filling reclamation. Scholars have conducted comprehensive research to assess the effectiveness of this application. Ma et al. [27] and Chen et al. [28] conducted analyses of the spatial and temporal changes in the nature of reclaimed soil and the reclamation effect brought about using coal gangue as a filling material. Jiao et al. [29] and Li et al. [30] revealed the changing patterns of bacterial diversity and community structure in the coal gangue-filled reclaimed land, as well as the relationship between these changes and soil physicochemical properties through high-throughput sequencing technology. Furthermore, Qiu et al. [31] and Yang et al. [32] investigated methods to enhance the quality of coal gangue-filled reclaimed land by incorporating fly ash and modified soil materials, thereby achieving the remediation of cadmium-contaminated soil. The studies of Xu et al. [33] and Chen et al. [34] elucidated the influence mechanism of temperature change on coal gangue-filled reclaimed soil. Fang et al. [35] and Song et al. [36] employed complex network theory to investigate the reconstruction mechanism and heavy metal distribution characteristics of coal gangue reclamation mine soil. Their findings provide a scientific basis for the safe utilization of coal gangue. Although ground filling reclamation is an effective method of coal gangue disposal, it is constrained by the complexity of land resources and manual intervention. Consequently, it is of paramount importance to identify novel approaches to coal gangue disposal.

In recent years, the filling of underground mining airspace has emerged as a novel approach to the disposal of coal gangue. In their respective works, Li [37] and Wang [38] provide comprehensive discussions on the efficient and harmless disposal and comprehensive resource utilization of coal gangue. They also emphasize the crucial role of underground filling technology in realizing the green mining of coal resources. Yang et al. [39] and Huang et al. [40] proposed a novel slurry filling technology based on the principles of coal-based solid waste underground filling and slurry pipeline transportation and developed a corresponding transportation model. He et al. [41] and Ju et al. [42] employed numerical simulation methods to investigate the damage characteristics and fracture evolution of coal gangue particles under varying pressure conditions. Gu et al. [43] and Zhu et al. [44,45] conducted comprehensive investigations into the flow characteristics and diffusion laws of gangue paste in underground filling spaces through similar simulations and industrial tests. Sun et al. [46] and Wu et al. [47] analyzed the mechanical properties and damage evolution mechanisms of coal gangue paste with high water content and viscosity using the acoustic emission, hydrodynamics, and discrete element coupling method (DEM-CFD). The studies provide theoretical support and practical guidance for the application of gangue underground filling technology. However, theoretical studies on the concentration of coal gangue paste filling pipeline transportation are still insufficient and require further exploration.

In view of this, based on the engineering background of coal gangue filling pipeline transportation (8 km) in a mine, based on the static anti-segregation performance and Bingham model, this paper determined the minimum concentration C_{wl} and the maximum concentration C_{wh} of coal gangue grout over the long distance, respectively, and constructed the calculation model of the ultra-long-distance concentration of coal gangue grout of different levels. At the same time, the functional relationship between the yield stress, plastic viscosity, and mass concentration of the coal gangue slurry of different grades is determined. In addition, the actual flow rate is modified by taking the maximum value function max, and the functional relationship between the actual flow rate and the mass concentration of coal gangue of different grades is obtained. The gradient range of the minimum concentration C_{wli}, the maximum concentration C_{whi}, and the concentration C_{wi} of coal gangue of different grades are calculated.

2. Methodology/Materials Used

2.1. Determine the Concentration Range of Different Grades of Gangue Slurry Ultra-Long-Distance Transportable Concentration Range

Reasonable gangue slurry quality concentration interval selection for the safety and stability of pipeline transportation is crucial. In ultra-long-distance transportation, the slurry must not only have good fluidity performance or not precipitate segregation but it must also ensure that the transport resistance meets the requirements of the existing equipment parameters of the mine and there is no pipeline clogging. Additionally, different grades of gangue slurry require different concentration intervals for transportation. Therefore, this paper, based on the static anti-dissociation performance, Bingham model, and the relationship between the mass concentrations, respectively, determines the gangue slurry ultra-long-distance transportable minimum concentration C_{wl} and gangue slurry ultra-long-distance transportable maximum concentration C_{wh}; it also proposes to establish different grades of gangue slurry ultra-long-distance transportable concentration calculation model $C_{wl} \leq C_w \leq C_{wh}$.

2.2. Ultra-Long-Distance Transportable Minimum Concentration of Gangue Slurry Based on Static Anti-Segregation Properties

The fine particles in the gangue slurry generally exhibit a "self-flocculation" effect, revealing the yield stress. Under static conditions, the coarse particles in the gangue slurry will not only bear the gravity G and buoyancy F_1 but also the slurry shear resistance F_2 [48–51]. To facilitate the analysis of the force state of the coarse particles in the gangue slurry, it is assumed to be an ideal and homogeneous solid spherical particle, radius r, as shown in the force analysis in Figure 1.
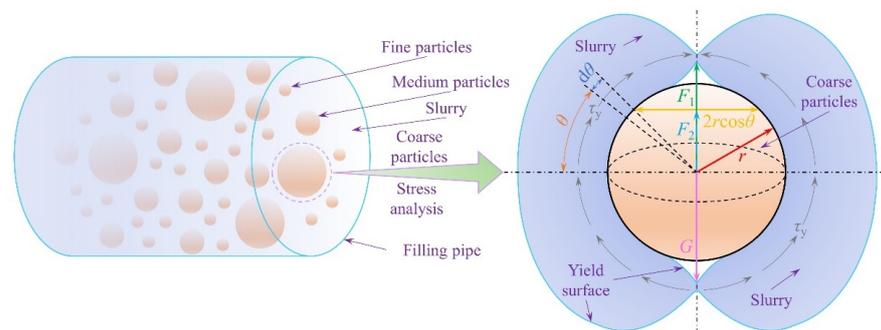
Figure 1. Static force analysis of coarse gangue particles.

Because gangue slurry contains a relatively large proportion of coarse particles, it settles easily and segregates when it encounters a minor shear resistance. Therefore, to prevent the settlement movement of coarse particles, the slurry's greatest shear resistance must satisfy the following requirements:

$$F_2 \geq \frac{\pi}{6} d^3 (\rho_s - \rho_m) g \tag{1}$$

where ρ_s is the bulk density of the coarse particles, in kg/m^3; ρ_m is the density of the gangue slurry, in kg/m^3; g is the acceleration of gravity, in m/s^2; and F_2 is the gangue slurry yield stress τ_y acting on the surface of the coarse particles caused by the shear resistance, in N.

If the differential area of the coarse particles at an angle θ with the horizontal is dA, then the differential area dA of the shear resistance F_2 in the vertical direction is

$$dF_2 = \tau_y \cos\theta dA = 2\pi r^2 \cos^2\theta \tau_y d\theta \tag{2}$$

Integrating Equation (2) gives the shear resistance of coarse particles in the gangue slurry:

$$F_2 = 4\pi r^2 \tau_y \int_0^{\frac{\pi}{2}} \cos^2 \theta d\theta = \frac{1}{4}\pi^2 d^2 \tau_y \tag{3}$$

Combining Equation (1) with Equation (3), we obtain the condition equation that the gangue slurry has anti-segregation performance under static conditions:

$$\frac{3\pi C \tau_s}{2(\rho_s - \rho_m)gd} \geq 1 \tag{4}$$

where τ_s is the static yield stress of gangue slurry, in MPa; C is the shear resistance coefficient, for the ideal smooth spherical particles, the value of 1.0, and for non-spherical particles, take 1.2–2.0; and d is the diameter of coarse particles; non-spherical particles should be used in the equivalent diameter $d_e = (6V/\pi)^{1/3}$, m.

Therefore, a model for calculating the minimum concentration of ultra-long-distance transportable gangue slurry based on the static anti-dissociation performance of different grades can be obtained:

$$f(C_{wli}) = M_{maxi} = \frac{3\pi C_i \tau_{si}}{2(\rho_s - \rho_{mi})gd_{maxi}} \tag{5}$$

where $i = (0, 1, 2, 3, 4, 5)$, $i = 0$ indicates that the amount of coarse particles in the gangue slurry is 0%, $i = 1$ indicates that the amount of coarse particles in the gangue slurry is 10%, and $i = 5$ indicates that the amount of coarse particles in the gangue slurry is 50%; C_i is the shear resistance coefficient of the i type gangue slurry; ρ_{mi} is the density of the i type gangue slurry, in kg/m^3; d_{maxi} is the i type of gangue slurry in the largest coarse particles in diameter, in m; C_{wli} is the i type of gangue slurry static segregation assessment value M_{maxi} corresponding to the mass concentration, so that $f(C_{wli}) = 1$ calculated C_{wli}, that is, the type of gangue slurry ultra-long-distance can be transported to the minimum concentration.

2.3. The Maximum Transportable Concentration of Coal Gangue Slurry in Ultra-Long Distance Based on Bingham Model

To ensure smooth transportation during gangue slurry filling, the flow rate must exceed the critical flow rate. Otherwise, solid particles will precipitate at the bottom of the pipe, leading to pipeline blockage. It is important to use subject-specific vocabulary when it conveys the meaning more precisely than a similar non-technical term. Fei Xiangjun's formula can estimate the critical flow rate v_c [52–54]:

$$v_c = \left[\frac{2gDC_v \cdot (\gamma_m - \gamma_j)\overline{\omega}}{e_s f \gamma_j} \right]^{1/3} \tag{6}$$

where g is the acceleration of gravity, in m/s^2; D is the inner diameter of the pipe, in m; C_v is the volume concentration of the gangue slurry; γ_m is the density of the gangue mixture, in t/m^3; γ_j is the density of the gangue slurry, in t/m^3; $\overline{\omega}$ is the average free settling velocity of the particles, in m/s; e_s is the suspension efficiency coefficient; and f is the Darcy resistance coefficient.

The following formula can be used to estimate a reasonable theoretical flow rate v_s, which should be the flow rate with a high conveying capacity, small water–sand ratio, and stable operation:

$$v_s = \frac{4Q_s}{3600\pi D^2} \tag{7}$$

where Q_s is the slurry flow rate, in m^3/h and D is the standard pipe diameter, in m.

To ensure smooth gangue slurry transport, the theoretical flow rate is usually more than 1.2 times the critical flow rate [55,56]. If the calculated theoretical flow rate of gangue

slurry is less than 1.2 times the critical flow rate, then the actual flow rate of gangue slurry v is set to 1.2 times the critical flow rate, as follows:

$$v = \max(1.2v_{\text{c}}, v_{\text{s}}) \tag{8}$$

For the rheological nature of structural flow gangue filling slurry, combined with the theoretical calculation formula of hydraulic gradient of the Bingham body [57,58], the Bingham model was used, and the calculation formula of hydraulic gradient was derived according to the Buckingham equation:

$$I = \frac{16}{3D} \cdot \tau + \frac{32v}{D^2} \cdot \mu \tag{9}$$

where I is the hydraulic gradient (resistance loss along the pipeline), in Pa/m; τ is the yield stress of the gangue slurry, in Pa; D is the inside diameter of the pipeline, in m; v is the actual flow rate of the pipeline, in m/s; and μ is the plastic viscosity of the slurry, in Pa·s.

For ease of calculation, the local resistance of the pipe is estimated as 8% of the resistance loss along the pipe to obtain the local resistance along all pipes:

$$I_{\text{j}} = 8\%I \tag{10}$$

where I_{j} is the local resistance loss of the pipeline, in Pa/m.

The total resistance of the gangue slurry transport pipeline can be derived as follows:

$$H_{\text{z}} = H_{\text{s}} + H_{\text{j}} + H_{\text{k}} \tag{11}$$

where H_{z} is the total resistance of the transportation of gangue slurry, that is, the working resistance of the pump body, in MPa; H_{s} is the total resistance of the horizontal straight section, in MPa; H_{j} is the local resistance of the slurry, in MPa; and H_{k} is the magnitude of resistance loss or drag reduction due to the elevation difference in slurry transportation, in MPa.

Substituting Equation (10) into Equation (11) can be derived from the gangue slurry for pipeline transportation resistance equation:

$$H_{\text{z}} = 1.08H_{\text{s}} + H_{\text{k}} \tag{12}$$

where the size of H_{k} depends on whether the filling pipeline slurry transport is downward or upward transport, that is, the filling station and filling location of the cavity relative relationship. When the elevation of the filling and mining area is greater than the elevation of the filling station, H_{k} is positive; when the elevation of the filling and mining area is less than the elevation of the filling station, H_{k} is negative.

By substituting Equation (9) into Equation (12), we can obtain the calculation model of the maximum concentration of coal gangue slurry that can be transported over a long distance based on the Bingham model:

$$f(C_{\text{wh}i}) = H_{\text{z}i} = 1.08 \cdot \left(\frac{16}{3D} \cdot \tau_i + \frac{32v_i}{D^2} \cdot \mu_i \right) \cdot l \pm \rho_{\text{m}i}gh \tag{13}$$

where $i = (0, 1, 2, 3, 4, 5)$, $i = 0$ when the mixing of coarse particles in the gangue slurry is 0%, $i = 1$ when the mixing of coarse particles in the gangue slurry is 10%, and $i = 5$ when the mixing of coarse particles in the gangue slurry is 50%; $C_{\text{wh}i}$ indicates that the i type of gangue slurry is the total resistance to the mass concentration of the corresponding $H_{\text{z}i}$; l is the pipeline conveying distance; $H_{\text{z}i}$ must be less than or equal to the maximum discharge pressure of the filling industrial pump and the difference between the starting pressure; and $H_{\text{z}i}$ takes the maximum value of the corresponding $C_{\text{wh}i}$, that is to say, the gangue slurry can be transported over long distances for the maximum concentration of gangue slurry.

2.4. Engineering Background for Transportable Concentration Modeling Parameters

The calculation of the ultra-long-distance transportable concentration of coal gangue slurry in this test is based on the engineering background of coal gangue filling pipeline transportation in a mine. The coal gangue slurry used in the filling of the mine is prepared by ball-milled coal gangue powder and roller-milled coal gangue powder (<3 mm), according to different water–cement ratios and different coarse particle content (i.e., different roller-milled coal gangue powder content; the content is 0, 10%, 20%, 30%, 40%, and 50%, respectively).

To elucidate the rationale behind varying the proportion of roller-milled gangue powder from 0% to 50%, a comprehensive analysis was conducted to consider both practical and technical considerations. At 0% roller-milled gangue powder, the objective was to understand the baseline properties and performance of the slurry system. Gradually increasing the proportion up to 50% allowed for the investigation of the impact of fine particle content on slurry viscosity, stability, and overall pipeline transportability. This range was selected because it allows for the observation of trends and the identification of optimal operating conditions while remaining within the practical limits of the roller milling process.

The pipeline transportation distance is 8 km, the height difference between the surface filling station and the underground goaf is 330 m, the inner diameter of the pipeline is 0.179 m, the maximum outlet pressure of the filling industrial pump is 18 MPa, the density of coal gangue is 2.63 t/m^3, and the annual processing capacity is 2 million tons. In order to determine the parameters of the calculation model of the ultra-long-distance transportable concentration of coal gangue slurry in the mine, the physical parameters and particle size range of two kinds of coal gangue powder were tested, and the rheological properties of coal gangue slurry with different grades were measured using the MCR72 rheometer from the Anton Paar Company, Austria. Table 1 displays the test scheme and related parameter results.

Table 1. Test scheme and related parameter results of different gradation coal gangue slurry.

No.	Coarse Particle Content /%	Water–Cement Ratio	Mass Concentration /%	Slurry Density ρ_{mi}/(t·m^{-3})	Static Yield Stress τ_{si}/Pa	1.2 Times Critical Flow Rate 1.2v_{ci}/(m·s^{-1})	Theoretical Flow Rate v_{si}/(m·s^{-1})	Actual Flow Rate v_i/(m·s^{-1})	Plastic Viscosity μ_i/(Pa·s)
C0-1		1:01	50	1.458	2.05	1.40	2.3	2.3	0.1079
C0-2	0	0.8:1	55.56	1.54	9.63	1.40	1.92	1.92	0.1969
C0-3		0.7:1	58.82	1.592	80.05	1.39	1.79	1.79	0.3758
C0-4		0.6:1	62.5	1.657	158.89	1.39	1.61	1.61	1.2063
C1-1		0.7:1	58.82	1.578	44.91	1.52	1.8	1.8	0.3169
C1-2	10	0.6:1	62.5	1.64	90.77	1.51	1.63	1.63	0.5616
C1-3		0.5:1	66.67	1.717	221.09	1.50	1.46	1.5	1.9284
C1-4		0.45:1	68.97	1.763	431.64	1.50	1.38	1.5	2.3311
C2-1		0.6:1	62.5	1.624	70.63	1.61	1.64	1.64	0.4437
C2-2	20	0.5:1	66.67	1.71	177.66	1.60	1.47	1.6	1.3423
C2-3		0.45:1	68.97	1.76	300.4	1.58	1.38	1.58	2.1113
C2-4		0.4:1	71.43	1.816	640.62	1.57	1.29	1.57	2.9661
C3-1		0.6:1	62.5	1.662	23.73	1.67	1.61	1.67	0.1053
C3-2	30	0.5:1	66.67	1.742	134.93	1.66	1.43	1.66	0.625
C3-3		0.4:1	71.43	1.838	443.16	1.63	1.27	1.63	2.3269
C3-4		0.35:1	74.07	1.893	1085.1	1.62	1.19	1.62	3.0143
C4-1		0.5:1	66.67	1.696	84.73	1.72	1.48	1.72	0.4044
C4-2	40	0.4:1	71.43	1.807	290.68	1.69	1.29	1.69	0.9209
C4-3		0.35:1	74.07	1.872	619.71	1.68	1.20	1.68	2.1673
C4-4		0.3:1	76.9	1.944	1640.4	1.66	1.11	1.66	2.9887
C5-1		0.5:1	66.67	1.758	62.06	1.75	1.42	1.75	0.1945
C5-2	50	0.4:1	71.43	1.854	208.78	1.73	1.26	1.73	0.6793
C5-3		0.35:1	74.07	1.909	460.98	1.72	1.18	1.72	1.2478
C5-4		0.3:1	76.9	1.97	1010.9	1.69	1.10	1.69	1.9734

2.5. Model Parameter Determination for the Minimum Transportable Concentration Calculation

The apparent density ρ_s of coal gangue particles is 2.63 t/m^3. Because the coal gangue particles belong to non-spherical particles, the shear resistance coefficients C_0, C_1, C_2, C_3, C_4, and C_5 of coal gangue slurry with different gradations are 1.5; the maximum particle size d_{max0} of coarse particles in coal gangue slurry with a coarse particle content of 0 is 2 mm; and the maximum particle sizes d_{max1}, d_{max2}, d_{max3}, d_{max4}, and d_{max5} of coarse particles in coal gangue slurry with a coarse particle content of 10%, 20%, 30%, 40%, and 50% are 2.36 mm.

The functional relationship between the static yield stress τ_{si}, density ρ_{mi}, and mass concentration C_{wi} of coal gangue slurry with different grades is shown in Figures 2 and 3, respectively.
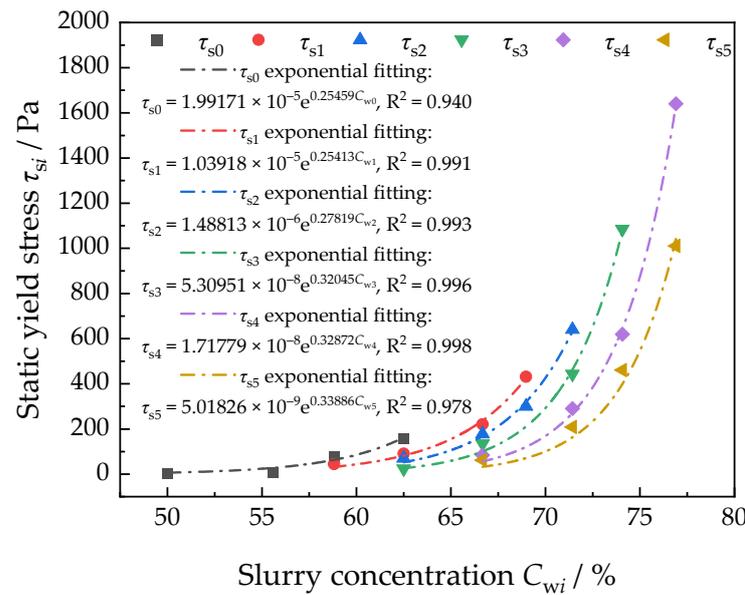
Figure 2. Relationship between static yield stress τ_{si} and mass concentration C_{wi} of coal gangue slurry with different gradations.
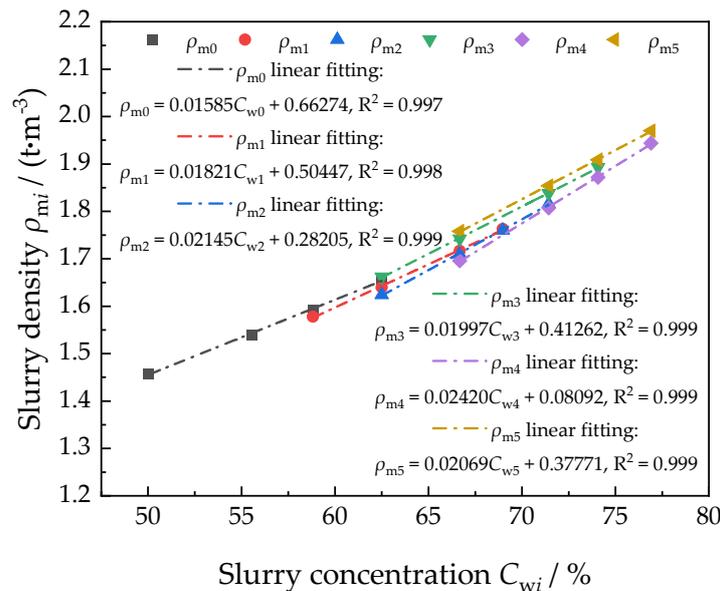
Figure 3. Relationship between density ρ_{mi} and mass concentration C_{wi} of coal gangue slurry with different gradations.

By organizing the above data and substituting them into Equation (5), the minimum transportable concentration calculation model can be simplified as follows:

$$\begin{cases} f(C_{wl0}) = \dfrac{3\pi C_0 \tau_{s0}}{2(\rho_s - \rho_{m0})g d_{max0}} = \dfrac{4.5\pi \times \left(1.99171 \times 10^{-5} e^{0.25459 C_{w0}}\right)}{39.2 \times (1.96726 - 0.01585 C_{w0})} \\[2mm] f(C_{wl1}) = \dfrac{3\pi C_1 \tau_{s1}}{2(\rho_s - \rho_{m1})g d_{max1}} = \dfrac{4.5\pi \times \left(1.03918 \times 10^{-5} e^{0.25413 C_{w1}}\right)}{39.2 \times (2.12553 - 0.01821 C_{w1})} \\[2mm] f(C_{wl2}) = \dfrac{3\pi C_2 \tau_{s2}}{2(\rho_s - \rho_{m2})g d_{max2}} = \dfrac{4.5\pi \times \left(1.48813 \times 10^{-6} e^{0.27819 C_{w2}}\right)}{39.2 \times (2.34795 - 0.02145 C_{w2})} \\[2mm] f(C_{wl3}) = \dfrac{3\pi C_3 \tau_{s3}}{2(\rho_s - \rho_{m3})g d_{max3}} = \dfrac{4.5\pi \times \left(5.30951 \times 10^{-8} e^{0.32045 C_{w3}}\right)}{39.2 \times (2.21738 - 0.01997 C_{w3})} \\[2mm] f(C_{wl4}) = \dfrac{3\pi C_4 \tau_{s4}}{2(\rho_s - \rho_{m4})g d_{max4}} = \dfrac{4.5\pi \times \left(1.71779 \times 10^{-8} e^{0.32872 C_{w4}}\right)}{39.2 \times (2.54908 - 0.02420 C_{w4})} \\[2mm] f(C_{wl5}) = \dfrac{3\pi C_5 \tau_{s5}}{2(\rho_s - \rho_{m5})g d_{max5}} = \dfrac{4.5\pi \times \left(5.01826 \times 10^{-9} e^{0.33886 C_{w5}}\right)}{39.2 \times (2.25229 - 0.02069 C_{w5})} \end{cases} \quad (14)$$

2.6. Model Parameter Determination for Maximum Transportable Concentration Calculation

In order to facilitate the analysis so that $\tau_i = \tau_{si}$, then the yield stress τ_i of different grades of gangue slurry and the mass concentration C_{wi} function of the relationship between the same Figure 2 are considered.

To determine the actual flow rate v_i of different grades of gangue slurry, the point-line diagrams of 1.2 times the critical flow rate 1.2 v_{ci}, theoretical flow rate v_{si}, and mass concentration C_{wi} of different grades of gangue slurry are plotted as shown in Figure 4.
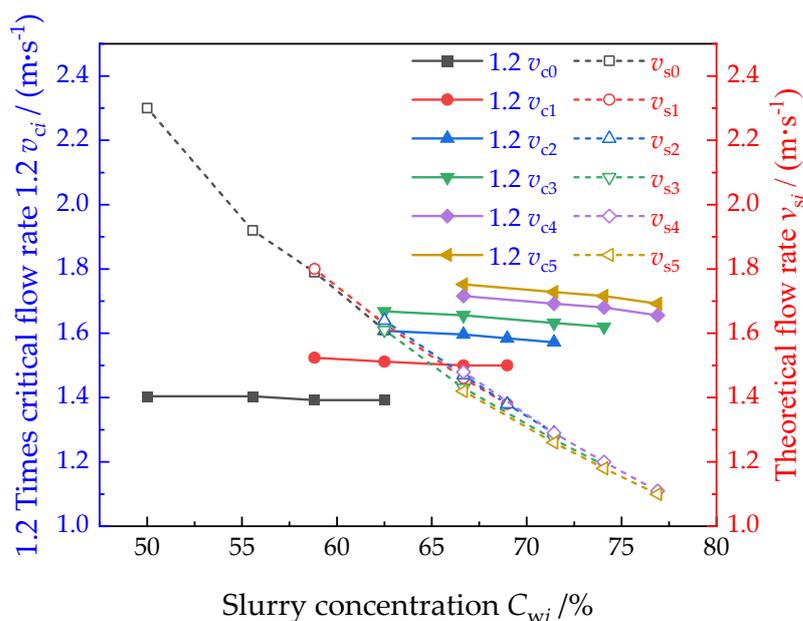
Figure 4. Relationship between 1.2 times the critical flow rate 1.2 v_{ci}, theoretical flow rate v_{si}, and mass concentration C_{wi} of coal gangue slurry with different gradations.

By taking the value function $v_i = \max(1.2\, v_{ci}, v_{si})$, the actual flow rate v_i of different grades of gangue slurry was obtained, and the functional relationship between the actual flow rate v_i and the mass concentration C_{wi} was fitted, as shown in Figure 5.

The plastic viscosity μ_i of the gangue slurries of different grades as a function of mass concentration C_{wi} is shown in Figure 6.
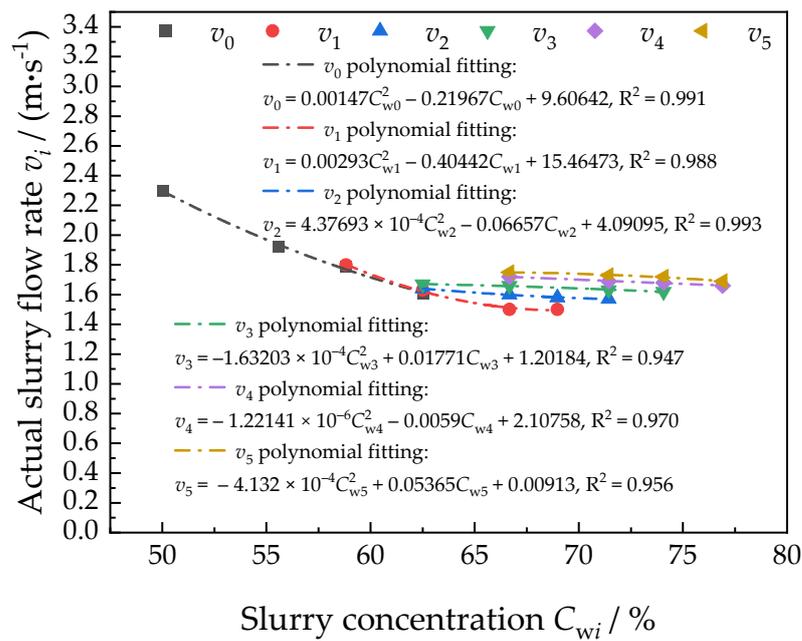
Figure 5. Relationship between actual flow rate v_i and mass concentration C_{wi} of coal gangue slurry with different gradations.
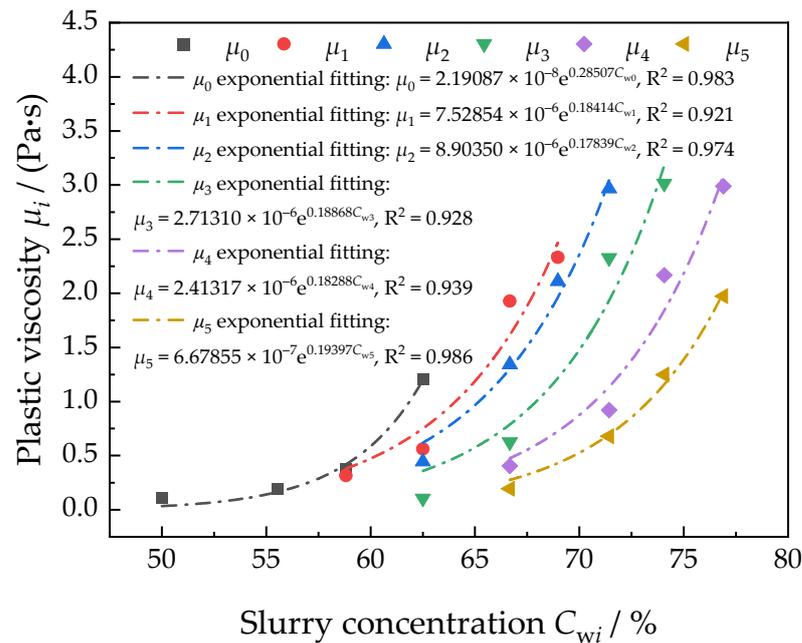
Figure 6. Relationship between plastic viscosity μ_i and mass concentration C_{wi} of coal gangue slurry with different gradations.

By organizing the above data and substituting them into Equation (13), the maximum transportable concentration calculation model can be simplified as follows:

$$\begin{cases}
f(C_{wh0}) = \frac{144l}{25D^2} \cdot (D \cdot \tau_0 + 6v_0 \cdot \mu_0) - \rho_{m0}gh = 1438157.361 \times [0.179 \times (1.99171 \times 10^{-5}e^{0.25459C_{w0}}) + \\
\quad 6 \times (9.60642 - 0.21967C_{w0} + 0.00147C_{w0}^2)(2.19087 \times 10^{-8}e^{0.28507C_{w0}})] - 3234 \times (0.66274 + 0.01585C_{w0}) \\
f(C_{wh1}) = \frac{144l}{25D^2} \cdot (D \cdot \tau_1 + 6v_1 \cdot \mu_1) - \rho_{m1}gh = 1438157.361 \times [0.179 \times (1.03918 \times 10^{-5}e^{0.25413C_{w1}}) + \\
\quad 6 \times (15.46473 - 0.40442C_{w1} + 0.00293C_{w1}^2)(7.52854 \times 10^{-6}e^{0.18414C_{w1}})] - 3234 \times (0.50447 + 0.01872C_{w1}) \\
f(C_{wh2}) = \frac{144l}{25D^2} \cdot (D \cdot \tau_2 + 6v_2 \cdot \mu_2) - \rho_{m2}gh = 1438157.361 \times [0.179 \times (1.48813 \times 10^{-6}e^{0.27819C_{w2}}) + \\
\quad 6 \times (4.09095 - 0.06657C_{w2} + 4.37693 \times 10^{-4}C_{w2}^2)(8.90350 \times 10^{-6}e^{0.17839C_{w2}})] - 3234 \times (0.28205 + 0.02145C_{w2}) \\
f(C_{wh3}) = \frac{144l}{25D^2} \cdot (D \cdot \tau_3 + 6v_3 \cdot \mu_3) - \rho_{m3}gh = 1438157.361 \times [0.179 \times (5.30951 \times 10^{-8}e^{0.32045C_{w3}}) + \\
\quad 6 \times (1.20184 + 0.01771C_{w3} - 1.63203 \times 10^{-4}C_{w3}^2)(2.71310 \times 10^{-6}e^{0.18868C_{w3}})] - 3234 \times (0.41262 + 0.01997C_{w3}) \\
f(C_{wh4}) = \frac{144l}{25D^2} \cdot (D \cdot \tau_4 + 6v_4 \cdot \mu_4) - \rho_{m4}gh = 1438157.361 \times [0.179 \times (1.71779 \times 10^{-8}e^{0.32872C_{w4}}) + \\
\quad 6 \times (2.10758 - 0.0059C_{w4} + 1.22141 \times 10^{-6}C_{w4}^2)(2.41317 \times 10^{-6}e^{0.18288C_{w4}})] - 3234 \times (0.08092 + 0.02420C_{w4}) \\
f(C_{wh5}) = \frac{144l}{25D^2} \cdot (D \cdot \tau_5 + 6v_5 \cdot \mu_5) - \rho_{m5}gh = 1438157.361 \times [0.179 \times (5.01826 \times 10^{-9}e^{0.33886C_{w5}}) + \\
\quad 6 \times (0.00913 + 0.05365C_{w5} - 4.132 \times 10^{-4}C_{w5}^2)(6.67855 \times 10^{-7}e^{0.19397C_{w5}})] - 3234 \times (0.37771 + 0.02069C_{w5})
\end{cases} \quad (15)$$

3. Results and Discussion

3.1. Prediction Results and Analysis of Minimum Transportable Concentration

As can be seen from Figure 2, the static yield stress τ_s of the gangue slurry of different grades and mass concentration C_{wi} data show an exponentially increasing trend. Under the same mass concentration, the more coarse particles are mixed, the lower the static yield stress is of the gangue slurry, thereby indicating that the more coarse particles are in gangue slurry, the more prone it is to sedimentation and segregation. Therefore, different levels of the gangue slurry ultra-long-distance transportable minimum concentration will increase with the increase in the content of coarse particles in the slurry, that is, the transportable minimum concentration should meet the $C_{wl0} < C_{wl1} < C_{wl2} < C_{wl3} < C_{wl4} < C_{wl5}$.

As can be seen from Figure 3, the density ρ_{mi} of different gangue slurry and the mass concentration C_{wi} data show a linear positive correlation. Through the linear function to fit the above data, the compound correlation coefficient of the fitted curve is greater than 0.99, which has a high fitting accuracy. Therefore, the density ρ_{mi} of the different gangue slurries will increase linearly with the increase in their mass concentration C_{wi}.

By taking the C_{wli} calculated with the parameters determined above, the minimum concentration of C_{wl0}, C_{wl1}, C_{wl2}, C_{wl3}, C_{wl4}, and C_{wl5} can be obtained from the ultra-long-distance transportable minimum concentration of the different graded gangue slurries in a mine, which are 47.30%, 50.56%, 53.18%, 56.26%, 58.39%, and 59.94%, respectively.

3.2. Prediction Results and Analysis of Maximum Transportable Concentration

As can be seen from Figure 4, when the amount of coarse particles in the gangue slurry is unchanged, the 1.2 times critical flow rate of the slurry will show a slightly decreasing trend as the mass concentration increases; at the same time, the more coarse particles are doped, the 1.2 times critical flow rate of the gangue slurry with different grades will show a gradient increase; in addition, the theoretical flow rate of different grades of the gangue slurry will be gradually reduced with the increase in the mass concentration. In the same mass concentration (in addition to group 1 and group 2 gangue slurry 1.2 times the critical flow rate of $1.2v_{c1}$, $1.2v_{c2}$, and the theoretical flow rate of v_{s1}, v_{s2} data), there is a crossover phenomenon; the rest of the group 1.2 times the critical flow rate of $1.2v_{ci}$ and the theoretical flow rate of v_{si} appear to be the phenomenon.

As can be seen from Figure 5, the actual flow rate v_i of gangue slurry with different grades and mass concentration C_{wi} shows a quadratic polynomial function relationship, and through the quadratic polynomial fitting of the data, it is found that except for the gangue slurry of the 3rd group, when the amount of coarse particles doped is 30%, the actual flow rate v_3 of gangue slurry and the slurry mass concentration C_{w3} fitted curve of the compound correlation coefficient is less than 0.95, and the rest of the groups of the compound correlation coefficient are more than 0.95.

As can be seen from Figure 6, the plastic viscosity μ_i of the gangue slurry of different grades is all increasing with the increase in mass concentration C_{wi}. Under the same mass concentration, the more coarse particles are doped, the smaller the plastic viscosity of

gangue slurry is, which indicates that the increase in coarse particle content in gangue slurry will reduce the viscosity of the slurry to a certain extent.

Through the parameters determined above, taking the $C_{\mathrm{wh}i}$ calculated then, it can be concluded that the maximum concentrations of $C_{\mathrm{wh}0}$, $C_{\mathrm{wh}1}$, $C_{\mathrm{wh}2}$, $C_{\mathrm{wh}3}$, C_{wh4}, and $C_{\mathrm{wh}5}$ of the different grades of gangue slurry ultra-long-distance transportable in a mine are 57.90%, 59.91%, 61.57%, 64.02%, 66.00%, and 67.90%, respectively.

3.3. Prediction Results and Analysis of Transportable Concentration Gradients

From Sections 3.1 and 3.2, it can be seen that when the dosage of coarse particles i is $0 \leq i \leq 5$ (i.e., the dosage of roller-mill gangue powder is 0–50%), the ultra-long-distance transportable minimum concentration $C_{\mathrm{wl}i}$ and the transportable maximum concentration $C_{\mathrm{wh}i}$ of different types of gangue slurry increase with the increase of the dosage of coarse particles i. Therefore, a scatter plot of the ultra-long-distance transportable minimum concentration $C_{\mathrm{wl}i}$ and the transportable maximum concentration $C_{\mathrm{wh}i}$ versus coarse particles I is plotted, and the above data are linearly fitted with the help of color filling to label the ultra-long-distance transportable concentration $C_{\mathrm{wl}i}$ of the gangue slurry of different grades of coal slurry. Therefore, the scatter plots of $C_{\mathrm{wh}i}$ and the dose of coarse particles i were plotted, and the linear fitting of the above data was performed. The gradient range of $C_{\mathrm{wl}i}$, the ultra-long-distance transportable concentration of different grades of gangue slurry, was marked with the help of color filling, as shown in Figure 7.
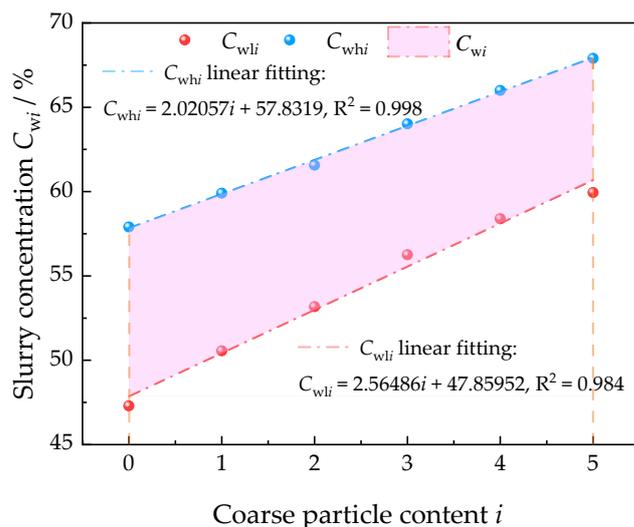
Figure 7. Relationship between the minimum transportable concentration $C_{\mathrm{wl}i}$, the maximum transportable concentration $C_{\mathrm{wh}i}$, and the coarse particle content i.

From Figure 7, it can be seen that when the coarse particle content i in the coal gangue slurry gradually increases, the minimum concentration $C_{\mathrm{wl}i}$ and the maximum concentration $C_{\mathrm{wh}i}$ of the ultra-long-distance transportable coal gangue slurry of different gradations show a linear increasing trend; after linear fitting, the multiple correlation coefficients are all greater than 0.98 and the slope of the fitting line of the minimum concentration $C_{\mathrm{wl}i}$ is 2.56 greater than the slope of the fitting line of the maximum concentration $C_{\mathrm{wh}i}$, which is 2.02; that is, the rising rate of the minimum concentration $C_{\mathrm{wl}i}$ is greater than the rising rate of the maximum concentration $C_{\mathrm{wh}i}$. It can be seen that with the increase of coarse particle content i, the $C_{\mathrm{w}i}$ gradient range of the ultra-long-distance transportable concentration of coal gangue slurry with different gradations gradually shrinks.

The transportable minimum concentration ($C_{\mathrm{wl}i}$) and maximum concentration ($C_{\mathrm{wh}i}$) of the coal gangue slurry can be calculated by fitting a straight line with the following values: when the coarse particle doping amount (i.e., the doping amount of the roller-mill gangue powder is 0, 10%, 20%, 30%, 40%, and 50%, respectively), the ultra-long-

distance transportable minimum concentration (C_{wl0}, C_{wl1}, C_{wl2}, C_{wl3}, C_{wl4}, and C_{wl5}) of the coal gangue slurry is 47.86%, 50.42%, 52.99%, 55.55%, 58.12%, and 60.68%, respectively; compared to the value of the minimum transportable concentration (C_{wli}) calculated in Section 2.5, the difference is only 0.56%, −0.14%, −0.19%, −0.27% and −0.74%, respectively. The ultra-long-distance transportable maximum concentration (C_{wh0}, C_{wh1}, C_{wh2}, C_{wh3}, C_{wh4}, and C_{wh5}) of the coal gangue slurry is 57.83%, 59.85%, 61.87%, 63.89%, 65.91%, and 67.93%, respectively; compared to the value of the maximum transportable concentration (C_{whi}) calculated in Section 2.6, the difference is only −0.07%, −0.06%, 0.30%, −0.13%, −0.09% and 0.03%, respectively.

It can be seen that the fitting accuracy in the above calculation model is good, which can provide theoretical support for the selection of the slurry quality concentration of the 8 km long-distance filling pipeline transportation of coal gangue slurry in this mine, and ensure that the slurry in the ultra-long-distance pipeline transportation does not occur under the settlement of segregation, siltation, and clogging.

Further, we can obtain the C_{wi} gradient of the ultra-long-distance transportation concentration of gangue slurry with different gradations in this mine as $47.86\% \leq C_{w0} \leq 57.83\%$, $50.42\% \leq C_{w1} \leq 59.85\%$, $52.99\% \leq C_{w2} \leq 61.87\%$, $55.55\% \leq C_{w3} \leq 63.89\%$, $58.12\% \leq C_{w4} \leq 65.91\%$, and $60.68\% \leq C_{w5} \leq 67.93\%$.

4. Conclusions

(1) In order to investigate the range of transportable concentrations of different grades of gangue slurry under ultra-long-distance transportation, based on the static anti-segregation performance and the Bingham model, respectively, the gangue slurry ultra-long-distance transportable minimum concentration of C_{wl} and the gangue slurry ultra-long-distance transportable maximum concentration of C_{wh} were determined, and the ultra-long-distance transportable concentration of different grades of gangue slurry was constructed as a model for calculating the concentration of different grades of gangue slurry.

(2) With a mine as the engineering background, different water–cement ratios and coarse particle content of the gangue slurry and rheological tests found that the yield stress of different grades of gangue slurry, plastic viscosity, and mass concentration follows the exponential function of the increasing law, and the density and slurry concentration of the mass of the linear function of the increasing law.

(3) With the help of taking the large value function max, comparing the size of 1.2 times the critical flow rate and the theoretical flow rate, taking the large value as the actual flow rate, and correcting the actual flow rate of pipeline transport via curve fitting, it was found that the actual flow rate of different grades of gangue slurry and the quality of the concentration were in accordance with the quadratic polynomial law of increase.

(4) According to the established transportable concentration calculation model, the minimum and maximum concentrations of gangue slurry with different coarse particle contents can be transported over a long distance, and the range of concentration of gangue slurry with different coarse particle contents can be transported over a long distance, which provides a method and theoretical support for the selection of concentration of filling slurry in long-distance pipeline transportation.

Author Contributions: Conceptualization, S.W., H.Y. and R.W.; methodology, S.W. and H.Y.; software, S.W. and R.W.; validation, S.W., H.Y., R.W., M.T., L.L., Y.L. and X.S.; formal analysis, S.W., H.Y. and M.T.; investigation, S.W., H.Y., L.L. and Y.L.; resources, S.W. and R.W.; data curation, S.W., H.Y. and R.W.; writing—original draft preparation, S.W., H.Y. and X.S.; writing—review and editing, S.W., H.Y. and R.W.; visualization, S.W. and M.T.; supervision, S.W., L.L., Y.L. and X.S.; project administration, S.W.; funding acquisition, S.W. All authors have read and agreed to the published version of the manuscript.

Appendix A

In this article, we use various symbols and nomenclature to denote different concepts and data. For the convenience and understanding of the readers, we have listed the explanations of all symbols and nomenclature in detail in Table A1 in Appendix A at the end of the paper. Readers can refer to this table for a clear understanding of the symbols and nomenclature used in the text.

Table A1. Explanation of all symbols and nomenclature.

Symbols and Nomenclature	Explanation
C_{wl}	Ultra-long-distance transportable minimum concentration
C_{wh}	Ultra-long-distance transportable maximum concentration
C_w	Ultra-long-distance transportable concentration
G	Gravity
F_1	Buoyancy
F_2	Slurry shear resistance
ρ_s	Bulk density of the coarse particles
ρ_m	Density of the gangue slurry
g	Acceleration of gravity
τ_y	Gangue slurry yield stress
τ_s	Static yield stress of gangue slurry
C	Shear resistance coefficient
d	Diameter of coarse particles
i	Amount of coarse particles in the gangue slurry
C_i	Shear resistance coefficient of the i type gangue slurry
ρ_{mi}	Density of the i type gangue slurry
d_{maxi}	i type of gangue slurry in the largest coarse particles in diameter
M_{maxi}	i type of gangue slurry static segregation assessment value
C_{wli}	i type of gangue slurry static segregation assessment value M_{maxi} corresponding to the mass concentration
v_c	Critical flow rate
g	Acceleration of gravity
D	Inner diameter of the pipe
C_v	Volume concentration of the gangue slurry
γ_m	Density of the gangue mixture
γ_j	Density of the gangue slurry
ω	Average free settling velocity of the particles
e_s	Suspension efficiency coefficients
f	Darcy resistance coefficient
v_s	Theoretical flow rate
Q_s	Slurry flow rate
v	Actual flow rate of gangue slurry
I	Hydraulic gradient (resistance loss along the pipeline)
τ	Yield stress of the gangue slurry
μ	Plastic viscosity of the slurry
I_j	Local resistance loss of the pipeline
H_z	Total resistance of the transportation of gangue slurry
H_s	Total resistance of the horizontal straight section
H_j	Local resistance of the slurry
H_k	Magnitude of resistance loss or drag reduction
H_{zi}	i type of total resistance of the transportation of gangue slurry
C_{whi}	i type of total resistance of the transportation of gangue slurry H_{zi} corresponding to the mass concentration
C_{wi}	i type of gangue slurry mass concentration
τ_i	i type of gangue slurry yield stress

References

1. Gosens, J.; Turnbull, A.B.H.; Jotzo, F. China's decarbonization and energy security plans will reduce seaborne coal imports: Results from an installation-level model. *Joule* **2021**, *6*, 782–815. [CrossRef]
2. Jiang, C.B.; Duan, M.K.; Yin, G.Z.; Wang, J.G.; Lu, T.Y.; Xu, J.; Huang, G.M. Experimental study on seepage properties, AE characteristics and energy dissipation of coal under tiered cyclic loading. *Eng. Geol.* **2017**, *221*, 114–123. [CrossRef]
3. Yang, Q.; Zhang, L.; Zou, S.H.; Zhang, J.S. Intertemporal optimization of the coal production capacity in China in terms of uncertain demand, economy, environment, and energy security. *Energy Policy* **2020**, *139*, 111360. [CrossRef]
4. Bian, Z.F.; Yu, H.C.; Han, X.T. Solutions to mine ecological restoration under the context of carbon. *J. China Coal Soc.* **2022**, *47*, 449–459.
5. Chen, X.; Xu, D.D.; Qian, Y.H.; Hong, X.P.; Liang, H.D. Pollution characteristics and toxicity assessment of PAHs in coal gangue from mine aera in Huaibei. *China Environ. Sci.* **2022**, *42*, 753–760.
6. Zhang, X.; Li, F.; Zhao, Q.L.; Li, X.J. Leaching characteristics and potential ecological risks of typical heavy metals in coal gangue. *J. China Coal Soc.* **2022**, *47*, 235–245.
7. Guo, S.J.; Zhang, J.X.; Li, M.; Zhou, N.; Song, W.J.; Wang, Z.J.; Qi, S.M. A preliminary study of solid-waste coal gangue based biomineralization as eco-friendly underground backfill material: Material preparation and macro-micro analyses. *Sci. Total Environ.* **2021**, *770*, 145241. [CrossRef] [PubMed]
8. Li, J.Y.; Wang, J.M. Comprehensive utilization and environmental risks of coal gangue: A review. *J. Clean. Prod.* **2019**, *239*, 117946. [CrossRef]
9. Zhang, H.L.; Shu, Y.X.; Yue, S.L.; Chen, Y.Q.; Mikulčić, H.; ur Rahman, Z.; Tan, H.Z.; Wang, X.B. Preheating pyrolysis-char combustion characteristics and kinetic analysis of ultra-low calorific value coal gangue: Thermogravimetric study. *Appl. Therm. Eng.* **2023**, *229*, 120583. [CrossRef]
10. Luo, C.; Li, S.; Ren, P.; Yan, F.; Wang, L.; Guo, B.; Ji, P. Enhancing the carbon content of coal gangue for composting through sludge amendment: A feasibility study. *Environ. Pollut.* **2024**, *348*, 123439. [CrossRef]
11. Shen, L.L.; Lai, W.A.; Zhang, J.X.; Sun, Z.H.; Li, M.; Zhou, N. Mechanical properties and micro characterization of coal slime water-based cementitious material-gangue filling: A novel method for co-treatment of mining waste. *Constr. Build. Mater.* **2023**, *408*, 133747. [CrossRef]
12. Zhang, J.X.; Zhou, N.; Gao, F.; Yan, H. Method of gangue grouting filling in subsequent space of coal mining. *J. China Coal Soc.* **2023**, *48*, 150–162.
13. Dong, C.X.; Wang, N.Q.; Li, J.S.; Chen, X.; Yan, X.S.; Ma, W. Mechanical properties and mechanism of co-curing saline soil with coal solid waste. *Coal Geol. Explor.* **2023**, *51*, 85–94.
14. Zhang, W.Q.; Chai, J.; Feng, X.J.; Dong, C.W.; Sun, Q.; Li, M.; Wang, L. Preparation and microstructure of coal gangue-based geopolymer. *J. China Univ. Min. Technol.* **2021**, *50*, 539–547.
15. Zhou, X.Y.; Guo, L.L.; Zhang, Y.B.; Wang, Z.H.; Ma, Y.; Li, X.F. Feasibility investigation of utilizing spontaneous combustion energy of abandoned coal gangue by constructing a novel artificial heat reservoir. *J. Clean. Prod.* **2022**, *373*, 133948. [CrossRef]
16. Wu, Q.; Tu, K.; Zeng, Y.F.; Liu, S.Q. Discussion on the main problems and countermeasures for building an upgrade version of main energy (coal) industry in China. *J. China Coal Soc.* **2019**, *44*, 1625–1636.
17. Cheng, Q.; Huang, G.; Zheng, J.; Liang, Q.M. New method for determining mode-i static fracture toughness of coal using particles. *Materials* **2024**, *17*, 1765. [CrossRef] [PubMed]
18. Mi, B.; Zhao, H.; Lu, M.; Zhou, Y.; Xue, Y.J. Synthesis of electrolytic manganese slag–solid waste-based geopolymers: Compressive strength and Mn immobilization. *Materials* **2024**, *17*, 1431. [CrossRef] [PubMed]
19. Ma, D.; Zhang, J.X.; Duan, H.Y.; Huang, Y.L.; Li, M.; Sun, Q.; Zhou, N. Reutilization of gangue wastes in underground backfilling mining: Overburden aquifer protection. *Chemosphere* **2021**, *264*, 128400. [CrossRef] [PubMed]
20. Guo, G.L.; Li, H.Z.; Zha, J.F. An approach to protect cultivated land from subsidence and mitigate contamination from colliery gangue heaps. *Process Saf. Environ.* **2019**, *124*, 336–344. [CrossRef]
21. Zheng, Y.F.; Cui, J.Y.; Gao, P.X.; Lv, J.F.; Chi, L.; Nan, H.Y.; Huang, Y.D.; Yang, F. Newly generated Ca-feldspar during sintering processes enhances the mechanical strength of coal gangue-based insulation bricks. *Materials* **2023**, *16*, 7193. [CrossRef] [PubMed]
22. Hu, Y.S.; Han, X.Y.; Sun, Z.Z.; Jin, P.; Li, K.L.; Wang, F.K.; Gong, J.W. Study on the reactivity activation of coal gangue for efficient utilization. *Materials* **2023**, *16*, 6321. [CrossRef] [PubMed]
23. Wang, H.; Zhang, F.J.; Ang, R.; Ren, D. Hydrothermal synthesis of cancrinite from coal gangue for the immobilization of Sr. *Materials* **2024**, *17*, 573. [CrossRef] [PubMed]
24. Yu, Z.X.; Jing, H.W.; Gao, Y.; Xu, X.; Zhu, G.F.; Sun, S.H.; Wu, J.Y.; Liu, Y.M. Effect of CNT-FA hybrid on the mechanical, permeability and microstructure properties of gangue cemented rockfill. *Constr. Build. Mater.* **2023**, *392*, 131978. [CrossRef]
25. Zhang, X.; Feng, X.P.; Wang, Z.P.; Jian, J.C.; Chen, S.; Luo, W.; Zhang, C. Experimental study on the physico-mechanical properties and microstructure of foam concrete mixed with coal gangue. *Constr. Build. Mater.* **2022**, *359*, 129428. [CrossRef]
26. Zhu, X.B.; Gong, W.H.; Li, W.; Bai, X.Y.; Zhang, C.X. Reclamation of waste coal gangue activated by Stenotrophomonas maltophilia for mine soil improvement: Solubilizing behavior of bacteria on nutrient elements. *J. Environ. Manag.* **2022**, *320*, 115865. [CrossRef] [PubMed]

27. Ma, T.H.; Li, R.; Wang, K.; Qu, J.F. Soil carbon dynamic characteristics of coal gangue-filled reclaimed cropland and forest land under time series. *Coal Sci. Technol.* **2023**, *51*, 260–268.

28. Chen, Y.C.; Zhao, P.; Zheng, L.G.; Jiang, C.L.; Yang, S.N. Temporal and spatial variation characteristics of soil fertility in coal mining subsidence reclamation area in Huainan Panyi mine. *Adm. Tech. Environ. Monit.* **2021**, *33*, 21–24.

29. Jiao, H.; Li, X.J. Variation in the soil bacterial community of reclaimed land filled with coal gangue. *J. China Coal Soc.* **2021**, *46*, 3332–3341.

30. Li, J.R.; Hou, H.P.; Wang, C.; Zhang, S.L.; Ma, J.; Ding, Z.Y.; Huang, L.; Dong, J.; Yang, Y.J. Soil bacteria diversity of reclaimed soil based on high throughput sequencing. *Environ. Sci. Technol.* **2018**, *41*, 148–157.

31. Qiu, J.J.; Zheng, L.G.; Chen, X.Y.; Chen, Y.C. Effects of fly ash incorporation on hydraulic characteristics and air permeability of coal gangue. *Environ. Eng.* **2021**, *39*, 131–137.

32. Yang, S.N.; Zhao, P.; Chen, Y.C.; An, S.K.; Zheng, L.G. Effect of modified vermiculite-montmorillonite on cadmium-contaminated soil in coal gangue filling and reclamation area. *Environ. Chem.* **2020**, *39*, 2777–2783.

33. Xu, L.J.; Zhu, X.M.; Liu, S.G.; Huang, C. Temporal and spatial response characteristics of reconstructed soil moisture under different particle size coal gangue temperature field. *J. China Coal Soc.* **2018**, *43*, 2304–2310.

34. Chen, M.; Chen, X.Y.; Gui, H.R.; Liu, G.J.; Liu, B.L.; Hu, Z.Y. Temperature variation and its response to topsoil thickness from reconstruction soil profile filled with coal gangue. *J. China Coal Soc.* **2017**, *42*, 3270–3279.

35. Li, F.; Li, X.J.; Hou, L.; Shao, A.R. A long-term study on the soil reconstruction process of reclaimed land by coal gangue filling. *Catena* **2020**, *195*, 104874.

36. Song, W.; Xu, R.P.; Li, X.J.; Min, X.Y.; Zhang, J.N.; Zhang, H.Z.; Hu, X.; Li, J.Y. Soil reconstruction and heavy metal pollution risk in reclaimed cultivated land with coal gangue filling in mining areas. *Catena* **2023**, *228*, 107147. [CrossRef]

37. Li, Q.H. Research progress on properties and comprehensive utilization of coal gangue. *Appl. Chem. Ind.* **2023**, *52*, 1576–1581.

38. Wang, Y.T. Status and prospect of harmless disposal and resource comprehensive utilization of solid waste of coal gangue. *Coal Geol. Explor.* **2022**, *50*, 54–66.

39. Yang, K.; Zhao, X.Y.; He, X.; Wei, Z. Basic theory and key technology of multi-source coal-based solid waste for green backfilling. *J. China Coal Soc.* **2022**, *47*, 4201–4216.

40. Huang, Y.C.; Duan, X.B.; Wang, Y.M.; Luo, H.T.; Hao, Y.X. Research on non-full pipeline flow transportation and prevention method of coal gangue cemented backfill. *Coal Sci. Technol.* **2020**, *48*, 117–122.

41. He, Z.Q.; Ju, F.; Xiao, M.; Ning, P.; Zhou, C.; Zhang, Y.Z.; Wang, D. Characterization of meso-deformation of gangue backfilling materials under cyclic loading. *J. Min. Saf. Eng.* **2022**, *39*, 1002–1010.

42. Ju, F.; Ning, P.; He, Z.Q.; Xiao, M.; Wang, G.W. Study on particle flow mesoscopic evolution law of coal gangue in compaction process. *J. Min. Saf. Eng.* **2020**, *37*, 183–191.

43. Gu, W.Z.; Yang, B.G.; Zhu, L.; Zhao, M.Y. Study on spatial characteristics of gangue slurry filling mining and engineering practice. *J. Min. Saf. Eng.* **2023**, *8*, 409–418.

44. Zhu, L.; Gu, W.Z.; Song, T.Q.; Pan, H.; Liu, Z.C.; Zhang, P.; He, Z.W. Research progress and prospect of coal gangue slurry backfilling technology in goaf. *Coal Sci. Technol.* **2023**, *51*, 143–154.

45. Zhu, L.; Pan, H.; Gu, W.Z.; Zhao, M.Y.; Zhang, X.F.; Xu, K. Experimental study on flow and diffusion law of gangue filling slurry in caving zone. *J. China Coal Soc.* **2021**, *46*, 629–638.

46. Sun, K.; Zhang, J.X.; He, M.C.; Li, M.; Wang, C.J.; Feng, W.C.; Li, F.M. Mechanical properties and damage evolution characteristics based on the acoustic emission of gangue and high-water-content materials based cemented paste backfill. *Constr. Build. Mater.* **2023**, *395*, 132324. [CrossRef]

47. Wu, B.Q.; Wang, X.D.; Liu, X.X.; Xu, G.G.; Zhu, S.B. Numerical simulation of erosion and fatigue failure the coal gangue paste filling caused to pumping pipes. *Eng. Fail. Anal.* **2022**, *134*, 106081. [CrossRef]

48. Jossic, L.; Magnin, A. Drag and stability of objects in a yield stress fluid. *Aiche J.* **2001**, *47*, 2666–2672. [CrossRef]

49. Beris, A.N.; Tsamopoulos, J.A.; Armstrong, R.C.; Brown, R.A. Creeping motion of a sphere through a Bingham plastic. *J. Fluid Mech.* **1985**, *158*, 219–244. [CrossRef]

50. Li, H.; Wu, A.X.; Wang, H.J.; Peng, N.B.; Jiao, H.Z. Static and dynamic anti-segregation property characterization of coarse-grained paste backfill slurry. *J. Central South. Univ. (Sci. Technol.)* **2016**, *47*, 3909–3915.

51. Wang, Z.H.; Qi, T.Y.; Feng, G.R.; Bai, J.W.; Pei, X.M.; Cui, B.Q.; Song, C.; Ran, H.Y. Electrical resistivity method to appraise static segregation of gangue-cemented paste backfill in the pipeline. *Int. J. Press. Vessel. Pip.* **2021**, *192*, 104385. [CrossRef]

52. Qiu, Y.Q. Analysis of Two Calculating Methods on the Drug Loss of Slurry Pipeline Transportation. *J. Gunzhou Univ. Technol. (Nat. Sci. Ed.)* **1999**, *28*, 31–35.

53. Zhao, L.A.; Cai, R.H.; Wang, T.L. Influence of coal slurry particle composition on pipeline hydraulic transportation behavior. *IOP Conf. Ser. Earth Environ. Sci.* **2018**, *113*, 012163. [CrossRef]

54. Wang, H.; Zhao, C.W.; Chen, S.C. Method for determining the critical velocity of paste-like slurry filling into goaf using computational fluid dynamics. *Arab. J. Geosci.* **2019**, *12*, 528. [CrossRef]

55. Wang, L.M.; Cheng, L.; Yin, S.H.; Yan, Z.P.; Zhang, X.L. Multiphase slurry flow regimes and its pipeline transportation of underground backfill in metal mine: Mini review. *Constr. Build. Mater.* **2023**, *402*, 133014. [CrossRef]

56. Gao, R.G.; Zhou, K.P.; Zhou, Y.L.; Yang, C. Research on the fluid characteristics of cemented backfill pipeline transportation of mineral processing tailings. *Alex. Eng. J.* **2020**, *59*, 4409–4426. [CrossRef]

57. Zhaidarbek, B.; Tleubek, A.; Berdibek, G.; Wang, Y.W. Analytical predictions of concrete pumping: Extending the Khatib–Khayat model to Herschel–Bulkley and modified Bingham fluids. *Cement Concrete Res.* **2023**, *163*, 107035. [CrossRef]

58. Denisenko, D.; Richard, G.L.; Chambon, G. A consistent three-equation shallow-flow model for Bingham fluids. *J. Non-Newton. Fluid* **2023**, *321*, 105111. [CrossRef]